

Ultrashort Mn-Mn Bonds in Organometallic Complexes

T. Alonso-Lanza (*),¹ J. W. González,¹ F. Aguilera-Granja,^{1,2} A. Ayuela¹

¹*Centro de Física de Materiales CFM-MPC CSIC-UPV/EHU,*

Donostia International Physics Center (DIPC),

Departamento de Física de Materiales,

Fac. de Químicas, UPV-EHU,

20018 San Sebastián, Spain

²*Instituto de Física, Universidad Autónoma de San Luis de*

Potosí, 78000 San Luis Potosí S.L.P., México

(Dated: March 6, 2024)

Manganese metallocenes larger than the experimentally produced sandwiched MnBz_2 compound are studied using several density functional theory methods. First, we show that the lowest energy structures have Mn clusters surrounded by benzene molecules, in so-called rice-ball structures. We then find a strikingly short bond length of 1.8 Å between pairs of Mn atoms, accompanied by magnetism depletion. The ultrashort bond lengths are related to Bz molecules caging a pair of Mn atoms, leading to a Mn-Mn triple bond. This effect is also found when replacing benzenes by other molecules such as borazine or cyclopentadiene. The stability of the Mn-Mn bond for Mn_2Bz_2 is further investigated using dissociation energy curves. For each spin configuration, the energy versus distance plot shows different spin minima with barriers, which must be overcome to synthesize larger Mn-Bz complexes.

Introduction

A number of organometallic compounds have been synthesized and used in a wide range of applications[1–5]. The synthesis of ferrocene[6–9] stimulated a search for related metallocenes, such as cobaltocene[10], nickelocene[11], rhodocene[12] and manganocene[13], in which a transition metal atom is located between two cyclopentadiene molecules. Similar compounds have been proposed combining transition-metal atoms with benzene molecules (TM-Bz compounds)[14]. The basic unit of such compound is a transition metal atom over a single Bz ring, known as a half-sandwich[15–17]. Such basic units can be combined to form larger compounds with either sandwich-like structures for early transition metals (Sc, Ti, and V) or rice-ball structures for late transition metals (Fe, Co, and Ni)[18]. TM-Bz compounds look promising for future applications. For instance, sandwich-like molecules have been proposed as conductors involving spin transport[19], either isolated bridging the tips of a Cu nanocontacts[19, 20] or pile up building infinite wires having Sc, Ti, V, Cr, and Mn[21]. Sandwiched molecules and infinite wires containing V, Nb, and Ta have been found to provide strong magnetic anisotropy [22]. We are interested in characterizing larger clusters with rice-ball structures, specifically in the study of Mn-Bz compounds, to gain knowledge on their still unfamiliar structures and properties.

The field of organometallics was recently boosted following a breakthrough in the synthesis of binuclear metallocenes, so-called dimetallocenes, such as decamethyldizincocene[23, 24] $\text{Zn}_2(\eta^5\text{C}_5\text{Me}_5)_2$ and $(\text{Zn}_2(\eta^5\text{C}_5\text{Me}_4\text{Et})_2)$. Compounds containing Mn with many nuclei have plenty of uses in organometallics[25]. Some previously described molecules containing Mn-C

bonds are dimanganese decacarbonyl[26–28] $\text{Mn}_2(\text{CO})_{10}$ and methylcyclopentadienyl manganese tricarbonyl $(\text{CH}_3\text{C}_5\text{H}_4)\text{Mn}(\text{CO})_3$, which has been used to increase the octane level of gasoline[29]. Experiments on TM-Bz compounds have been performed, leading to their synthesis in the gas phase and their characterization using spectroscopic methods [18, 30–32] and in magnetic experiments[33, 34]. TM-Bz compounds are present in many types of molecular clusters. Small Mn-Bz compounds, such as MnBz_2 , have been synthesized[18, 35]. As for Mn adatoms in graphene, Mn sandwiched between Bz molecules prefers to be in a hollow position[36, 37]. Theoretical studies are required to understand larger complexes of inner Mn clusters surrounded by Bz molecules as to be produced experimentally.

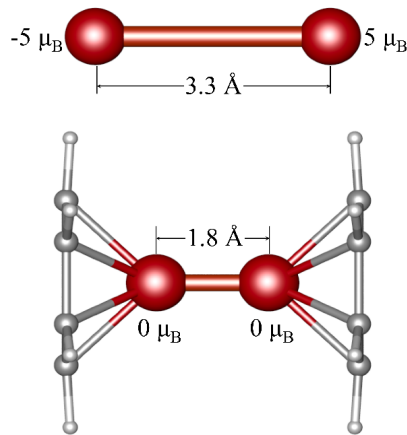


FIG. 1: Scheme showing the ultrashort bond effect in Mn surrounded by benzene molecules. Note the large reduction in Mn-Mn distance and the total quenching of the magnetic moment.

Dimetalloenes and multimetalloenes have been largely investigated using density functional theory (DFT) calculations. Different external molecules have been considered, such as Bz, cyclopentadiene, and even fullerenes[38]. Similarly, many different central metal atoms have been studied, leading to alkaline-earth dimetalloenes[39–42], transition metal dimetalloenes[43–45], heterodinuclear compounds[46, 47] and zinc isoelectronic elements, such as Cd and Hg [48]. Although multinuclear metallocenes of Co, Cu, and Ni, and other transition metals have been described [43–45, 49–54], the study of larger manganese benzene compounds is still to be done.

We herein investigate organometallic compounds in which Bz molecules cage clusters with a few Mn atoms, Mn_nBz_m . The benzene molecules strongly affect the bonding between manganese atoms, differently to other transition metals. Manganese benzene compounds are also interesting because they are in the middle between two trends, sandwich-like structures for early transition metals and rice-ball structures for late transition metals [18]. We find that the clusters contain Mn-Mn multiple (triple) bonds with ultrashort interatomic distances and depleted magnetism. We then focus on the electronic structure of the smaller Mn_2Bz_2 molecule to further improve our understanding of such molecules. The two Bz molecules covering the Mn_2 molecule appear to stabilize a non-magnetic local minimum in the inner Mn dimer. We verify that these results also appear when replacing the caging benzenes with other molecules. Furthermore, ultrashort bonds are also found in larger Mn-Bz compounds, indicating that the effect is robust and that strong dimerization is induced in larger molecules. Because most of experiments work with charged clusters, we have checked that positively charged Mn-Bz clusters also present ultrashort Mn-Mn bonds. Lastly we study the synthesis of the Mn_2Bz_2 molecule, as a first step towards larger Mn-Bz compounds, and we show that different high local spin magnetic moment states create barriers to such syntheses.

I. RESULTS AND DISCUSSION

A. Metallization induced superdimerization

The ground state geometries of the Mn_2Bz_2 , Mn_3Bz_3 , Mn_4Bz_3 , and Mn_4Bz_4 molecules are shown in Fig. 2. We also consider the roles of isomers for each cluster, and study other geometries and magnetic solutions. We first determine whether a sandwich or rice-ball structure is preferred. The rice-ball geometry has lower energy for each of the four Mn-Bz clusters studied here. The results for the sandwich structures are shown in the Supplemental Material. We perform calculations for several isomers with different magnetic moments. For instance, a symmetric Mn_3Bz_3 isomer with $5 \mu_B$ has an energy difference of 1 eV from the ground state, and a distorted Mn_3Bz_3

isomer with $7 \mu_B$ lies 0.5 eV higher in energy. All the isomers are lying higher in energies than the structures presented in Fig. 2.

All the ground state molecules have strikingly short bond lengths between the Mn couples. The Mn_2Bz_2 molecule is the simplest system to show this effect with a Mn-Mn distance of 1.8 Å. The ultrashort bond lengths are unexpected because larger distances between Mn atoms have been reported, such as 3.4 Å for the Mn dimer[55–57], 2.93 Å for dimanganese decacarbonyl[26, 28], 2.4–2.6 Å for manganese carbides[58, 59] and the broad distance range of 2.25–2.95 Å for several Mn bulk allotropes [57]. On the other hand, analogous short multiple bonds have been shown theoretically and experimentally for other transition metals, such as in ultrashort Cr dimers (1.73 Å) within organic molecules [60].

We focus on the locally unpolarized Mn_2Bz_2 molecule with a Mn-Mn distance of around 1.8 Å. The loss of magnetism is a hallmark of the ultrashort bonds between Mn atoms capped with Bz molecules. The magnetic moments of irregular systems, such as Mn_3Bz_3 and Mn_4Bz_3 , are almost depleted. In the unit consisting of a Mn atom over a benzene molecule, the magnetic moment decreases from $5 \mu_B$ to $3 \mu_B$ [16]. However, the total elimination of the magnetism for the Mn_2Bz_2 molecule is still surprising.

When combining two Mn_2Bz_2 units to form a Mn_4Bz_4 molecule, the larger compound also has ultrashort bonds, and the total and local magnetic moments remain zero. The Bz molecules around the Mn atoms form a distorted tetrahedron, tilted because of neighboring Bz rings. There are two short bond lengths of 1.94 Å and four larger bond lengths of 2.56 Å. The short bond lengths are between the opposite atom pairs, labeled 1-2 and 3-4 in Fig. 2.

The two cases Mn_2Bz_2 and Mn_4Bz_4 have ultrashort distances and total magnetism depletion. The ultrashort Mn-Mn bonds also occurs for other molecules, such as Mn_3Bz_3 and Mn_4Bz_3 . The Mn_3Bz_3 ground state geometry depletes most of the magnetism, and gives an ultrashort distance of 1.88 Å between Mn(1) and Mn(3). The third Mn atom, Mn(2), moves away and remains bonded mainly to Mn(1), with a bond length of 2.22 Å. The side position of Mn(2) bends the Bz molecule associated with Mn(1). The total spin magnetic moment is $1 \mu_B$, localized mainly on Mn(2) with $1.53 \mu_B$. The Mn(1) atom has antiferromagnetic coupling with a magnetic moment of $-0.57 \mu_B$, and the Mn(3) local moment decreases to a very small value of $0.28 \mu_B$. [86] The added Mn-Bz unit distorts the Mn_2Bz_2 geometry, giving nonzero local magnetic moments on the Mn atoms. The peculiar distorted structure is due to the large energy gain because of the ultrashort Mn-Mn bond. The ultrashort bond phenomenon is therefore found partially for Mn_3Bz_3 . The dimerized Mn_4Bz_4 and Mn_3Bz_3 structures indicate that the ultrashort bond mechanism is caused by two Mn atoms caged by Bz molecules.

We next consider when the short Mn-Mn bonds accompanied by magnetism quenching occur by removing

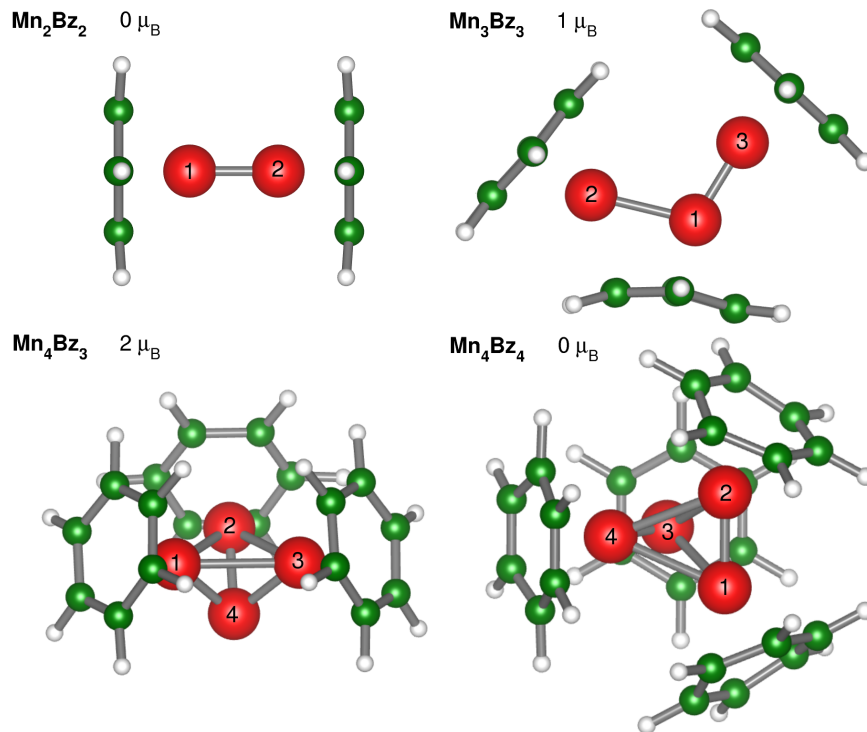


FIG. 2: Geometries of the Mn_mBz_n molecules studied here. Mn, C, and H atoms are shown as red, green and white spheres, respectively. Note that the total spin magnetic moment is null or small for all cases.

a Bz molecule from an already dimerized structure. We consider Mn_4Bz_3 molecule shown in Fig. 2. The structure is obtained by removing a Bz molecule from the final Mn_4Bz_4 geometry, and fully relaxing the geometry again. The Mn_4Bz_3 molecule becomes reorganized because the Mn(4) atom has lost its Bz molecule. The Mn(1), Mn(2) and Mn(3) atoms form an equilateral triangle with sides 2.62 Å. The Mn(4) atom is bonded to the other three Mn atoms with short bond lengths of 2.05 Å, which are larger than those found in Mn_4Bz_4 . In this case, the local magnetic moments are antiferromagnetically coupled, with small values of $1.07 \mu_B$ for Mn(1), Mn(2) and Mn(3) and $-0.83 \mu_B$ for Mn(4). Most of carbon atoms have a negative induced magnetic moment of 0.02–0.03 μ_B . Although the local manganese magnetism is reduced and the bonds are short, it seems that the presence of two Bz molecules caging two Mn atoms is key to the ultrashort Mn-Mn bond scheme.

We now consider the stability these compounds to discuss their possible synthesis. We compute the formation energy, per manganese atom, for Mn_nBz_m clusters toward separated Mn atoms and Bz molecules, using the expression $E_f = (n E_{\text{Mn}} + m E_{\text{Bz}} - E_{\text{total}})/n$. We find that the formation energies are always favorable, in the range 1.76–2.18 eV. Furthermore, the HOMO-LUMO gaps are in the range 1.17–0.72 eV. Taking into account the well-known issue of gap underestimation for generalized gradient approximation, the gap values suggest that the molecules are stable. The gap narrows as the size of

the molecule increases. We could have followed the series by looking for larger molecules with ultrashort Mn-Mn bonds, such as Mn_5Bz_5 , Mn_6Bz_6 , and so on. Nevertheless, it appears that placing five or more Bz rings around a nucleus of larger Mn clusters is a real challenge due to the lack of space.

Molecular beam experiments use charged systems, therefore we determine how our neutral Mn-Bz clusters are affected when positively charged. An electron was removed from the structures, which were fully relaxed again. The results show there are two different trends depending on the size. Smaller clusters, Mn_2Bz_2^+ and Mn_3Bz_3^+ preserve the ultrashort distance of the Mn-Mn bonds. Note that the Mn_2Bz_2^+ cluster now has a magnetic moment of 1 μ_B and that the Mn_3Bz_3^+ increases from 1 μ_B for the neutral case to 2 μ_B . Larger complexes, Mn_4Bz_3^+ and Mn_4Bz_4^+ lost the ultrashort Mn-Mn bond distance and display bulk-like behavior. The Mn-Mn distances increases to values within the interval 2.3–2.6 Å. The local magnetic moments of Mn increase to values within the range 2.0 – 3.5 μ_B and the Mn atoms are antiferromagnetically coupled.

We further test when ultrashort Mn-Mn bonds would appear by replacing the caging benzenes with other organic molecules, such as cyclopentadiene C_5H_6 , and even inorganic molecules, such as borazine $\text{B}_3\text{H}_6\text{N}_3$ [61–63]. After careful atomic relaxations, both types of caging compounds for Mn_2 present ultrashort Mn-Mn bonds accompanied by magnetism depletion. [87] Then, the ultra-

short Mn-Mn bond effect, accompanied by a significant decrease in the magnetic moment of Mn, seems to be robust, and it is expected to be found for other molecules caging manganese atoms.

B. Simplest case: Mn_2Bz_2

We focus on the smaller Mn_2Bz_2 molecule to investigate the ultrashort Mn-Mn bond, also found in larger molecules. The fully relaxed Mn_2Bz_2 molecule has an unexpected Mn-Mn bond length of 1.8 Å, as shown in Fig. 2. However, the Mn dimer has been found to be stabilized by van der Waals interactions [55] and to have a bond length of more than 3 Å. Bulk metallic Mn is predicted to have interatomic distances of between 2.25 Å and 2.95 Å, depending on the allotropic structure. The Mn-Mn distance decreases when shifting from van der Waals-like bonds to metallic-like bonds. However, our results are surprising because the Mn-Mn bonds can be ultrashort. This means that the Mn-Mn bonding mechanism in hybrid Mn-Bz molecules is different from the one seen in Mn clusters and bulk Mn [56]. We find a non-magnetic solution for the Mn_2Bz_2 molecule that contrasts with the high-spin solutions obtained from most DFT calculations for the Mn dimer [56, 57, 64–67]. Benzene molecules reduce spin-splitting in the Mn atoms, and electrons fill the minority-spin bonding molecular orbitals instead of the majority-spin antibonding molecular orbitals. The ultrashort Mn-Mn distance is therefore related to the loss of magnetism. For spin-compensated solutions, the Mn dimer in Mn_2Bz_2 can be further compressed because electrons between the Mn atoms suffer less electronic repulsion when they fill the same Mn-Mn molecular levels with opposite spins. Note that high-spin solutions for Mn_2Bz_2 require larger distances because of the larger electronic repulsion between Mn levels.

To improve our understanding of the ultrashort Mn-Mn bonds, we carry out spin-polarized single point calculations for the Mn_2Bz_2 molecule. The Mn atoms are separated by 0.1 Å in each step, and the Bz rings are maintained in the same relative positions with respect to the Mn atoms. We plot the energy against Mn-Mn distance in Fig. 3(a). The local magnetic moments of Mn are zero up to a distance of 2.4 Å, and there is a deep minimum at a distance of 1.8 Å. The energy increases sharply by more than 2 eV as the Mn atoms separate. Two different DFT codes gives the minimum at 1.8 Å, even when the Mn_2Bz_2 molecule is distorted and allowed to relax again. The large energy gain is associated to the multiple (triple) bond between Mn atoms, as shown by considering the molecular orbitals and electron localization function, as described in the Supplemental Material.

We further explore the nature of Mn_2Bz_2 bonding to determine when both inner Mn atoms are locally spin-compensated. We study the isolated Mn_2 molecule, varying the Mn-Mn distance from 1 Å to 4 Å, as shown in Fig. 3(b). When the magnetization is released, the total

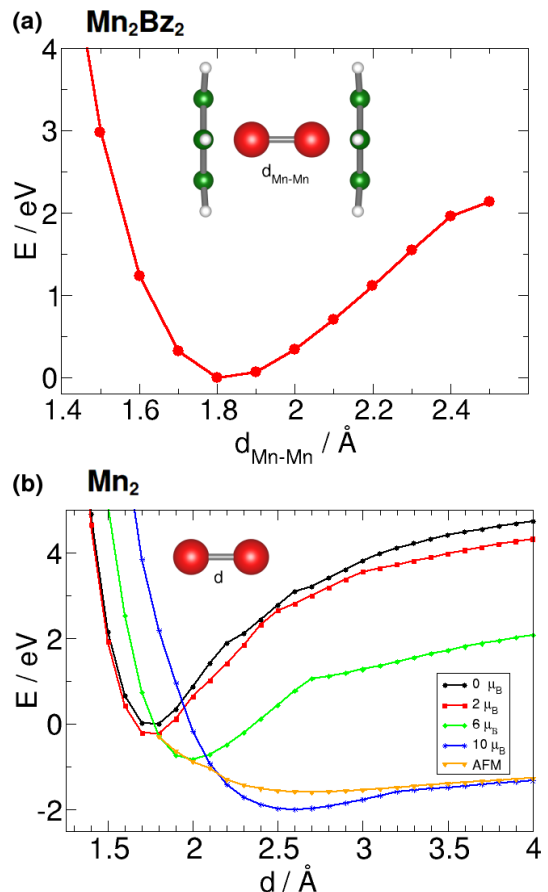


FIG. 3: (a) Total energy versus Mn-Mn bond length for the Mn_2Bz_2 cluster. (b) Total energy versus distance for the Mn_2 dimer. Each curve has the total magnetic moment fixed at a different value.

magnetic moment varies from 2 μ_B for distances shorter than 1.7 Å to 10 μ_B for distances larger than 2.4 Å. We have also calculated the energy versus distance curves for fixed total spin values of 0, 2, 6, and 10 μ_B . We find that each spin curve has a different minimum. The global minimum for Mn_2 is around 2.5 Å, as previously reported at this level of calculations (LDA/GGA)[64–67]. The antiferromagnetic curve is almost degenerated to that of 10 μ_B for long distances, in agreement with previous calculations[68]–[88]. The strong Mn-Mn bonding in the Mn_2 molecule at short distances can therefore be computed accurately enough using generalized gradient approximation (GGA) functionals. The low spin solutions (with 0 and 2 μ_B) shrink to local minima at bond lengths of about 1.8 Å, as reported previously [69, 70]. The minimum at short distances is also favored in the bonding in Mn_2Bz_2 because the magnetic moment in the 3d Mn levels is decreased by the Bz molecules, so the Mn-Mn distances are dramatically reduced.

C. Implications for the synthesis of Mn_2Bz_2

The MnBz_2 molecule has been synthesized and identified using spectroscopic techniques in the same way as for other TM-Bz compounds [18]. Larger Mn-Bz compounds are, however, difficult to synthesize [71]. It seems that electron spin restrictions may prevent their synthesis. Here, we investigate the path for the synthesis of Mn_2Bz_2 by estimating energy barriers. The possible barriers are extracted from the energy versus Bz-Bz distance curves for different total magnetic moments, as shown in Fig. 4. Further computational details are given in the Supplemental Material. The total magnetic moment decreases from long to short distances, and a barrier appears as the Mn_2Bz_2 molecule forms at high spin. We can overcome this barrier by, for instance, bringing the Mn-Mn core into a low spin state sandwiched between distant Bz molecules. We propose that using thermal or optical pumping techniques on the Mn cluster and Bz molecule precursors could help to find routes for synthesizing the Mn_2Bz_2 molecule and larger Mn-Bz clusters.

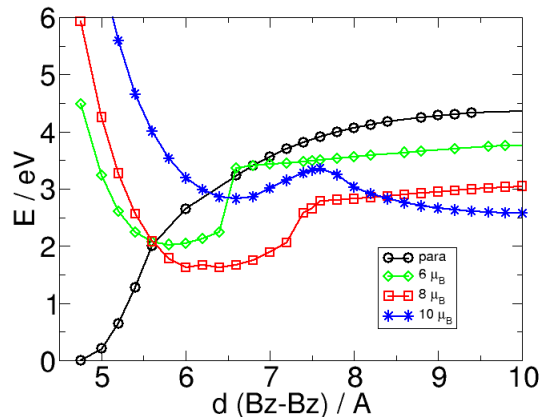


FIG. 4: Mn_2Bz_2 total energies for different distances between the benzene molecules. The curves were obtained by fixing the total magnetic moment.

II. FINAL REMARKS

We studied Mn-Bz molecules with rice-ball configurations. We found a multiple (triple) bond between the inner manganese atoms in the core metal cluster. Two hallmarks of this effect are a strikingly short Mn-Mn bond length of about 1.8 Å and a lack of magnetism. These can be explained because every two Bz molecules stabilize the two neighboring Mn atoms with no spin polarization. Furthermore, other molecules such as borazine and cyclopentadiene have a similar effect on manganese atoms. We also found that the ground states of larger molecules, such as Mn_3Bz_3 and Mn_4Bz_4 , stabilize the irregular structures of the molecules with ultrashort Mn-Mn bonds. Last, we investigated the roles of differ-

ent spins, looking at the Mn_2Bz_2 energy as the Bz-Bz distance varied. There are energy barriers that could be overcome by canceling local Mn spins using optical or thermal techniques. These results suggest that further experimental progress can be made in synthesizing larger Mn-Bz clusters that are of interest in the field of organometallic compounds.

III. COMPUTATIONAL DETAILS

We performed DFT calculations using the Vienna ab-initio simulation package (VASP), based on the projected augmented wave method (PAW) [72, 73]. For the exchange and correlation functionals we used the Perdew-Burke-Ernzenhof (PBE) form of the generalized gradient approximation (GGA) [74]. We chose a cubic unit cell with sides 30 Å in order to avoid interaction between images. We used an electronic temperature of 25 meV and a cutoff energy of 500 eV. The Mn-Bz molecules were relaxed until the forces were less than 0.006 eV/Å. The results obtained using VASP were reproduced using the SIESTA package within a GGA and applying the PBE functional for selected cases. We used a mesh cut-off of 250 Ry and sampled at the Γ -point. The atomic cores were described using nonlocal norm-conserving relativistic Troullier-Martins [75] pseudopotentials with non-linear core corrections factorized in the Kleyman-Bylander form. The basis set size was double zeta plus polarization orbitals with an energy shift of 0.05 eV. Using the SIESTA package, the same minima were obtained for the Mn_2Bz_2 and Mn_3Bz_3 molecules.

Acknowledgments

This work was partially supported through projects FIS2013-48286-C02-01-P and FIS2016-76617-P funded by the Spanish Ministry of Economy and Competitiveness MINECO, by the Basque Government under the ELKARTEK project (SUPER), and by the University of the Basque Country (Grant No. IT-756-13). TALL acknowledges a grant provided by the MPC Material Physics Center - San Sebastián. FA-G acknowledges the DIPC for their generous hospitality. The authors also acknowledge the support of the DIPC computer center.

Supplemental Material: Ultrashort Mn-Mn Bonds in Organometallic Complexes

SI. Mn-Mn BOND IN Mn_2Bz_2

A. Molecular orbitals

We studied the hybridization of the six p_z molecular orbitals of benzene (Bz) and the $3d$ shell of Mn. The properties of benzene orbitals are well known. Three of the four valence electrons of each carbon atom are used to build strong σ bonds with neighboring C and H atoms. The extra electrons in the p_z orbitals of C atoms form delocalized π bonds, which are related to the aromaticity of Bz. These p_z electrons are higher in energy than σ electrons and close to the HOMO level, and are responsible for the reactivity of Bz with other atoms and molecules. The six p_z orbitals are involved in the six well-known molecular orbitals. Some molecular orbitals are degenerated and are divided into four types: σ (π_1), π (π_2, π_3), δ (π_4^*, π_5^*) and ϕ (π_6^*). For Mn_2Bz_2 , the degenerate Bz levels are, however, split in energy because the Bz molecules are slightly bent toward the Mn atoms.

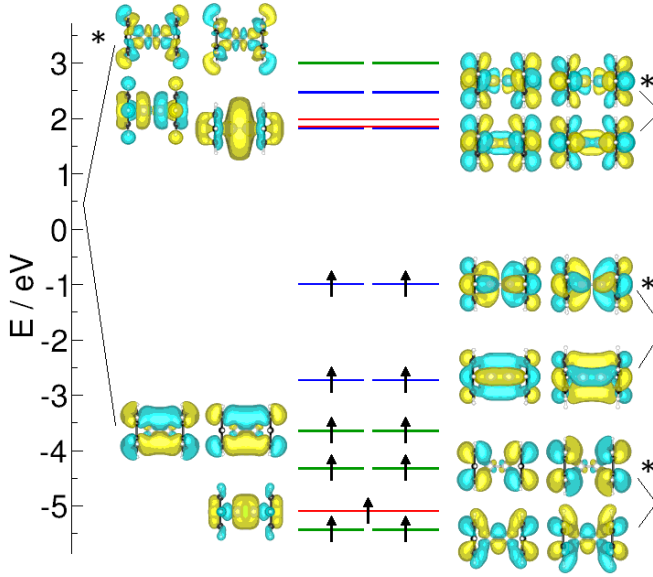


FIG. S1: Energy levels and wave-functions near the Fermi energy. The colors of the levels denote the molecular orbital types: σ in red, π in green, and δ in blue. Antibonding molecular orbitals are marked with asterisks.

In the presence of a Bz molecule, the Mn $3d$ orbitals split into three different energies, according to the orbital symmetry, in the energy order $d\sigma$ ($3d_{z^2}$), $d\pi$ ($3d_{xz}, 3d_{yz}$), and $d\delta$ ($3d_{xy}, 3d_{x^2-y^2}$). The Mn orbitals hybridize with the Bz orbitals when they have the same symmetry, to produce σ , π and δ molecular orbitals, as has been found in similar analyses [84, 85]. The Mn $3d_{z^2}$ orbitals are not

expected to interact much with the Bz because they point toward the center of the Bz ring. Regarding the Mn $4s$ orbitals, σ bonds with the Bz π_1 molecular orbitals are expected.

The energy levels for Mn_2Bz_2 near the Fermi energy are shown in Fig. S1. The σ , π , and δ molecular orbitals are found by considering the number of nodal planes, (0, 1, and 2, respectively). The two π orbitals have lower energies than the δ orbitals, and are occupied by more electrons. Figure S1 shows that the π and δ molecular orbitals have bonding or antibonding character that alternates as the energy increases. The number of hybrid orbitals expected in each symmetry can also be explained. For π symmetry, there are four π orbitals from two Bz molecules and four $3d$ orbitals ($3d_{xz}$ and $3d_{yz}$ from each atom). As a result, there are eight molecular orbitals. The same argument can be applied to the δ orbitals.

To summarize, a spin compensated structure was found with electrons filling the σ , π and δ hybrid molecular orbitals built from the Bz p_z levels and Mn $3d$ levels, following symmetry considerations. Therefore, the ultrashort Mn-Mn bond is a triple bond, with σ , π and δ bonds.

B. Electron localization function

The Mn-Mn bond is studied in detail using the electron localization function, as shown in Fig. S2. There is a direct σ metallic bond between the Mn atoms, composed of $3d_{z^2}$ orbitals. The disk around the bond center indicates the presence of π and δ molecular orbitals and bonds. The basins in the Mn-Mn bonds have an electron localization function value of 0.125, which is small and typical of metallic bonds. The electron localization function results agree completely with the energy levels, hybridization, and wave-functions described above, confirming the triple-bond characteristics of the bonds between the Mn atoms.

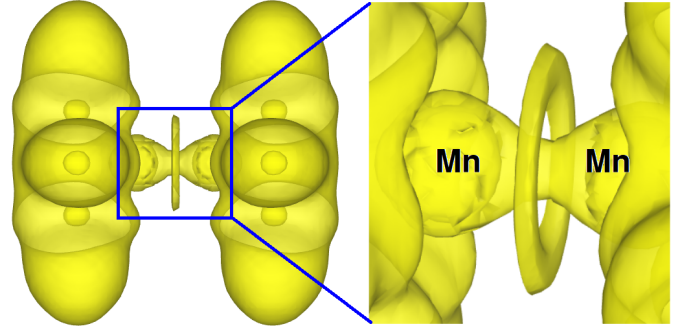


FIG. S2: (Left) Electron localization function for the Mn_2Bz_2 molecule cut at a value of 0.125. (Right) An expanded view of the highlighted part of the left figure.

SII. ENERGY BARRIERS

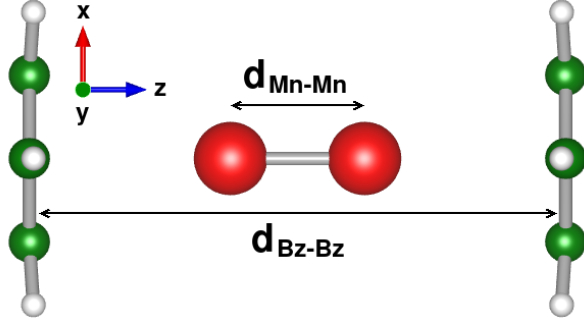


FIG. S3: Scheme of the geometry used for the barrier calculations.

We next comment on the barrier that prevents the formation of the Mn_2Bz_2 molecule. We carried out calculations for Mn_2Bz_2 for a set of spin magnetic moments and distances. The energy barrier is calculated using the geometrical arrangement shown in Fig. S3. The total magnetic moment is fixed to 0, 6, 8, and $10 \mu_B$. For each spin value, the molecule is computed using several Bz-Bz distances $d_{\text{Bz-Bz}}$ between 4.8 and 10 Å at steps of 0.2 Å. The C and H atoms are relaxed in the xy plane, keeping the Bz-Bz distance frozen. For each calculation, the Mn atoms are initially set in the center with a distance $d_{\text{Mn-Mn}}$ of 2 Å, as shown in Fig. S3. The Mn atoms are allowed to relax along the z axis. For large $d_{\text{Bz-Bz}}$ values, the Mn atoms can either bind to Bz molecules or form a Mn-Mn core in the center. These two geometries explain the abrupt step seen for some energy curves in Fig. 4 in the main article, for instance at 6.4 Å for $6 \mu_B$, and at 7.2 Å for $8 \mu_B$. At these distances, the Mn-Mn forces are at maxima, and for larger distances the Mn-Mn atoms prefer to bond together remaining separated from the Bz molecules.

SIII. Mn-Bz SANDWICHES

We also considered sandwiched structures for the four Mn-Bz clusters, as shown in Fig. S4. The rice-ball structures presented in the main text are more stable than the sandwiched structures, with energy differences larger than 1 eV. Furthermore, the total magnetic moments are larger for the sandwiched structures than for the rice-ball structures.

SIV. Mn-Bz: CHARGE STATE

We studied local charges using the Mulliken scheme within the SIESTA package. For the Mn_2Bz_2 molecule,

there is a small charge transfer of 0.18 electrons from each Mn atom towards C atoms. For Mn_3Bz_3 , the charge

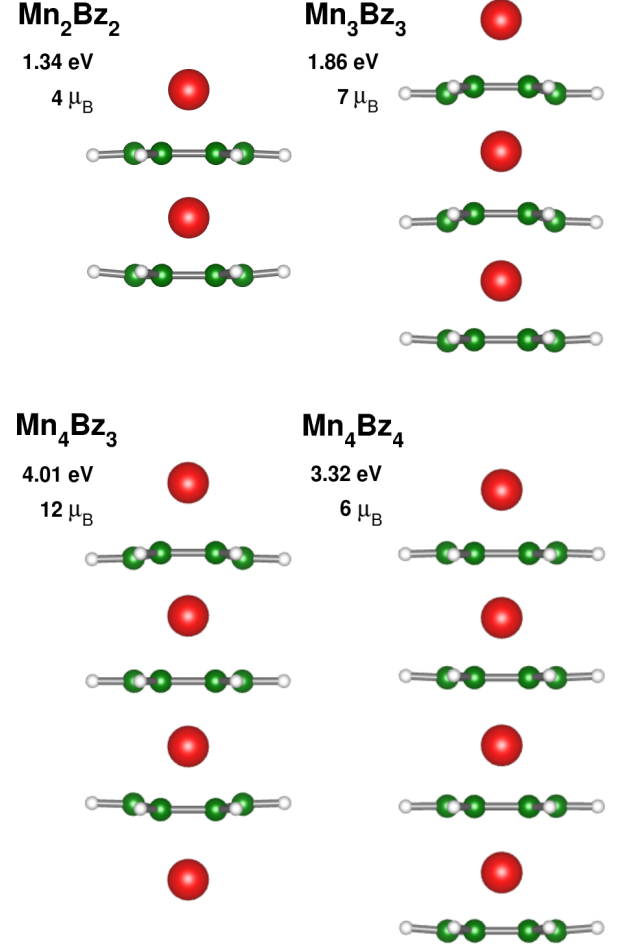


FIG. S4: Sandwich-like isomers of the four different Mn-benzene clusters studied. The energy difference with respect to the corresponding rice-ball structure and the total magnetic moment for each cluster are included.

transfers of Mn(1) and Mn(2) are almost negligible, and the charge transfer reaches a threshold of 0.11 electrons for Mn(3). For Mn_4Bz_3 , Mn(1), Mn(2), and Mn(3) lose 0.07 electrons each, and Mn(4) gains 0.42 electrons; globally each Mn atom therefore receives 0.21 electrons from Bz molecules. For Mn_4Bz_4 , each Mn atom gains almost 0.04 electrons, meaning that, in total, 0.16 electrons move from Bz molecules to Mn atoms. We therefore find that increasing the Mn cluster size causes the charge transfer between Mn atoms and Bz molecules to change sign. In general, charge transfer values are small. We can assume that the Mn oxidation state is zero for the calculated Mn-Bz clusters, and specifically for the ultrashort Mn-Mn bond in Mn_2Bz_2 .

- [1] R. H. Crabtree, *The organometallic chemistry of the transition metals* (John Wiley & Sons, 2009).
- [2] I. Omae, *Applications of organometallic compounds* (Wiley, 1998).
- [3] J. Kollonitsch, *Ann. New York Acad. Sci.* **125**, 161 (1965).
- [4] M. P. Coogan, P. J. Dyson, and M. Bochmann, *Organometallics* **31**, 5671 (2012).
- [5] J. F. Harrod and R. M. Laine, *Applications of Organometallic Chemistry in the Preparation and Processing of advanced materials*, vol. 297 (Springer Science & Business Media, 2012).
- [6] T. Kealy and P. Pauson, *Nature* **168**, 1039 (1951).
- [7] S. A. Miller, J. A. Tebbboth, and J. F. Tremaine, *J. Chem. Soc.* pp. 632–635 (1952).
- [8] J. Dunitz, L. Orgel, and A. Rich, *Acta Crystallogr.* **9**, 373 (1956).
- [9] H. Werner, *Angew. Chem. Int. Ed.* **51**, 6052 (2012).
- [10] R. Liu, S.-H. Ke, W. Yang, and H. U. Baranger, *Cobaltocene as a spin filter* (2007).
- [11] W. Pfab and E. Fischer, *Z. Anorg. Allg. Chem.* **274**, 316 (1953).
- [12] F. Cotton, R. Whipple, and G. Wilkinson, *J. Am. Chem. Soc.* **75**, 3586 (1953).
- [13] G. Wilkinson and F. Cotton, *Tech. Rep.*, Harvard Univ. (1954).
- [14] K. M. Wedderburn, S. Bililign, M. Levy, and R. J. Gdanitz, *Chem. Phys.* **326**, 600 (2006).
- [15] R. Pandey, B. K. Rao, P. Jena, and M. A. Blanco, *J. Am. Chem. Soc.* **123**, 3799 (2001).
- [16] R. Pandey, B. Rao, P. Jena, and J. M. Newsam, *Chem. Phys. Lett.* **321**, 142 (2000).
- [17] R. Muhida, W. Agerico Diño, M. Mahmudur Rahman, H. Kasai, and H. Nakanishi, *J. Phys. Soc. Jpn.* **73**, 2292 (2004).
- [18] T. Kurikawa, H. Takeda, M. Hirano, K. Judai, T. Arita, S. Nagao, A. Nakajima, and K. Kaya, *Organometallics* **18**, 1430 (1999).
- [19] M. Ormaza, N. Bachellier, M. N. Faraggi, B. Verlhac, P. Abufager, P. Ohresser, L. Joly, M. Romeo, F. Scheurer, M.-L. Bocquet, et al., *Nano Lett.* (2017).
- [20] M. Karolak and D. Jacob, *J. Phys. Condens. Matter* **28**, 445301 (2016).
- [21] H. Xiang, J. Yang, J. Hou, and Q. Zhu, *J. Am. Chem. Soc.* **128**, 2310 (2006).
- [22] Y. Mokrousov, N. Atodiresei, G. Bihlmayer, and S. Blügel, *Int. J. Quantum Chem.* **106**, 3208 (2006).
- [23] I. Resa, E. Carmona, E. Gutierrez-Puebla, and A. Monge, *Science* **305**, 1136 (2004).
- [24] A. Grirrane, I. Resa, A. Rodriguez, E. Carmona, E. Alvarez, E. Gutierrez-Puebla, A. Monge, A. Galindo, D. del Río, and R. A. Andersen, *J. Am. Chem. Soc.* **129**, 693 (2007).
- [25] G. Cahiez, C. Duplais, and J. Buendia, *Chem. Rev.* **109**, 1434 (2009).
- [26] E. Brimm, M. Lynch Jr, and W. Sesny, *J. Am. Chem. Soc.* **76**, 3831 (1954).
- [27] R. King, J. Stokes, and T. Korenowski, *J. Organomet. Chem.* **11**, 641 (1968).
- [28] L. F. Dahl, E. Ishishi, and R. Rundle, *J. Chem. Phys.* **26**, 1750 (1957).
- [29] J. M. Davis, *Environ. Health Persp.* **106**, 191 (1998).
- [30] M. A. Duncan, *Int. J. Mass spectrom.* **272**, 99 (2008).
- [31] W. Zheng, S. N. Eustis, X. Li, J. M. Nilles, O. C. Thomas, K. H. Bowen, and A. K. Kandalam, *Chem. Phys. Lett.* **462**, 35 (2008).
- [32] J. Buchanan, G. Grieves, J. Reddic, and M. Duncan, *Int. J. Mass Spectrom.* **182**, 323 (1999).
- [33] K. Miyajima, S. Yabushita, M. B. Knickelbein, and A. Nakajima, *J. Am. Chem. Soc.* **129**, 8473 (2007).
- [34] S. T. Akin, V. Zamudio-Bayer, K. Duanmu, G. Leistner, K. Hirsch, C. Bulow, A. Lawicki, A. Terasaki, B. v. Issendorff, D. G. Truhlar, et al., *J. Phys. Chem. Lett.* **7**, 4568 (2016).
- [35] V. Zamudio-Bayer, K. Hirsch, A. Langenberg, M. Kosick, A. Lawicki, A. Terasaki, B. v. Issendorff, and J. T. Lau, *J. Chem. Phys.* **142**, 234301 (2015).
- [36] H. Sevinçli, M. Topsakal, E. Durgun, and S. Ciraci, *Phys. Rev. B* **77**, 195434 (2008).
- [37] Y. Mao, J. Yuan, and J. Zhong, *J. Phys. Condens. Matter* **20**, 115209 (2008).
- [38] G. Gao, X. Xu, and H. S. Kang, *J. Comput. Chem.* **30**, 978 (2009).
- [39] P. K. Chattaraj, D. R. Roy, and S. Duley, *Chem. Phys. Lett.* **460**, 382 (2008).
- [40] Y.-H. Kan, *J. Mol. Struct. THEOCHEM* **894**, 88 (2009).
- [41] Q. S. Li and Y. Xu, *J. Phys. Chem. A* **110**, 11898 (2006).
- [42] A. Velazquez, I. Fernández, G. Frenking, and G. Merino, *Organometallics* **26**, 4731 (2007).
- [43] J. Zhou, W.-N. Wang, and K.-N. Fan, *Chem. Phys. Lett.* **424**, 247 (2006).
- [44] H. Zhu, Y. Chen, S. Li, X. Yang, and Y. Liu, *Int. J. Hydrogen Energy* **36**, 11810 (2011).
- [45] Y. Meng, Y. Han, H. Zhu, Z. Yang, K. Shen, B. Suo, Y. Lei, G. Zhai, and Z. Wen, *Int. J. Hydrogen Energy* **40**, 12047 (2015).
- [46] N. He, H.-b. Xie, and Y.-h. Ding, *J. Phys. Chem. A* **112**, 12463 (2008).
- [47] H. Hu, L. Zang, W. Zhang, and X. Li, *Comp. Theor. Chem.* **1058**, 41 (2015).
- [48] E. Carmona and A. Galindo, *Angew. Chem. Int. Ed.* **47**, 6526 (2008).
- [49] B. Rao and P. Jena, *J. Chem. Phys.* **116**, 1343 (2002).
- [50] G. E. Froudakis, A. N. Andriotis, and M. Menon, *Chem. Phys. Lett.* **350**, 393 (2001).
- [51] X. Zhang and J. Wang, *J. Phys. Chem. A* **112**, 296 (2008).
- [52] I. Valencia, G. Tavizón, N. Barba-Behrens, and M. Castro, *Chem. Phys.* **390**, 51 (2011).
- [53] J. Kua and K. M. Tomlin, *J. Phys. Chem. A* **110**, 11988 (2006).
- [54] J. W. Gonzalez, T. Alonso-Lanza, F. Delgado, F. Aguilera-Granja, and A. Ayuela, *Phys. Chem. Chem. Phys.* **19**, 14854 (2017).
- [55] S. Yamamoto, H. Tatewaki, H. Moriyama, and H. Nakano, *J. Chem. Phys.* **124**, 124302 (2006).
- [56] S. Nayak, B. Rao, and P. Jena, *J. Phys. Condens. Matter* **10**, 10863 (1998).
- [57] C. Baumann, R. Van Zee, S. Bhat, and W. Weltner Jr, *J. Chem. Phys.* **78**, 190 (1983).
- [58] X. Chong, Y. Jiang, R. Zhou, and J. Feng, *Comput. Mater. Sci.* **87**, 19 (2014).

- [59] P. Karen, H. Fjellvag, A. Kjekshus, and A. Andresen, *Acta Chem. Scand.* **45**, 549 (1991).
- [60] F. R. Wagner, A. Noor, and R. Kempe, *Nat. Chem.* **1**, 529 (2009).
- [61] L. Zhu and J. Wang, *J. Phys. Chem. C* **113**, 8767 (2009).
- [62] P. Li, Z. Yang, W. Zhang, and S. Xiong, *J. Mol. Struct.* **1038**, 1 (2013).
- [63] G. Wilkinson, F. Cotton, and J. Birmingham, *J. Inorg. Nucl. Chem.* **2**, 95 (1956).
- [64] M. Qing-Min, X. Zun, L. Ying, and L. You-Cheng, *Chin. Phys. Lett.* **24**, 1908 (2007).
- [65] P. Bobadova-Parvanova, K. Jackson, S. Srinivas, and M. Horoi, *J. Chem. Phys.* **122**, 14310 (2005).
- [66] R. Longo, E. Noya, and L. Gallego, *Phys. Rev. B* **72**, 174409 (2005).
- [67] M. Kabir, A. Mookerjee, and D. Kanhere, *Phys. Rev. B* **73**, 224439-1 (2006).
- [68] D. Tzeli, U. Miranda, I. G. Kaplan, and A. Mavridis, *J. Chem. Phys.* **129**, 154310 (2008).
- [69] A. Wolf and H.-H. Schmidtke, *Int. J. Quantum Chem.* **18**, 1187 (1980).
- [70] S. Paul and A. Misra, *J. Mol. Struct. THEOCHEM* **907**, 35 (2009).
- [71] T. Yasuike, A. Nakajima, S. Yabushita, and K. Kaya, *J. Phys. Chem. A* **101**, 5360 (1997).
- [72] P. E. Blöchl, *Phys. Rev. B* **50**, 17953 (1994).
- [73] G. Kresse and D. Joubert, *Phys. Rev. B* **59**, 1758 (1999).
- [74] J. P. Perdew, K. Burke, and M. Ernzerhof, *Phys. Rev. Lett.* **77**, 3865 (1996).
- [75] N. Troullier and J. L. Martins, *Phys. Rev. B* **43**, 1993 (1991).
- [76] J. Mejía-López, A. H. Romero, M. E. Garcia, and J. Morán-López, *Phys. Rev. B* **78**, 134405 (2008).
- [77] M. D. Morse, *Chem. Rev.* **86**, 1049 (1986).
- [78] F. López-Urías and A. Díaz-Ortiz, *Phys. Rev. B* **68**, 180406 (2003).
- [79] S. Yamanaka, T. Ukai, K. Nakata, R. Takeda, M. Shoji, T. Kawakami, T. Takada, and K. Yamaguchi, *Int. J. Quantum Chem.* **107**, 3178 (2007).
- [80] M. Cheeseman, R. Van Zee, H. Flanagan, and W. Weltner Jr, *J. Chem. Phys.* **92**, 1553 (1990).
- [81] J.-C. Rivoal, J. S. Emampour, K. J. Zeringue, and M. Vala, *Chem. Phys. Lett.* **92**, 313 (1982).
- [82] R. Van Zee, C. Baumann, and W. Weltner Jr (1981).
- [83] K. Bier, T. Haslett, A. Kirkwood, and M. Moskovits, *J. Chem. Phys.* **89**, 6 (1988).
- [84] M. Karolak and D. Jacob, *J. Phys. Condens. Matter* **28**, 445301 (2016).
- [85] T. Yasuike and S. Yabushita, *J. Phys. Chem. A* **103**, 4533 (1999).
- [86] Small spin polarization is induced in the C atoms (0.06 μ_B being the highest value for one C atom) with opposite sign to the closest Mn atom.
- [87] For the cyclopentadiene-caged Mn_2 , the ultrashort Mn-Mn distance is 1.85 Å. The Mn local magnetic moments become about 0.1 μ_B , which are not fully depleted in comparison to Bz-Mn molecule because a H atom from cyclopentadiene is bound to a Mn atom. For the borazine-caged Mn_2 , the Mn-Mn distance is 1.82 Å and the local and total magnetic moments are fully depleted.
- [88] There is a delicate balance between exchange and splitting, and small changes in distance can modify the magnetic characteristics of the Mn dimer[76]. Although DFT has been shown to be successful for many systems, the choice of exchange correlation functionals is key for some systems, such as the Mn dimer. Note, for example, that obtaining the minimum caused by van der Waals interactions[56, 77, 78] at distances larger than 3 Å requires using hybrid functionals[79] or even the CASSCF (Complete Active Space Self-Consistent Field) method[55], which reproduces the antiferromagnetic coupling and the bond length larger than 3 Å obtained in experiments[57, 80–83].